

Supporting Information for:

Microscopic Insights into Poly- and Mono-Crystalline Methane

Hydrate Dissociation in Na-Montmorillonite Pores at Static and

Dynamic Fluid Conditions

Bin Fang^a, Tao Lü^{b,c}, Wei Li^d, Othonas A. Mourtos^e, Thijs J.H. Vlugt^e, Fulong Ning^{d,f*}

^a School of Mathematics and Physics, China University of Geosciences, Wuhan 430074, China

^b School of Automation, China University of Geosciences, Wuhan 430074, China

^c Hubei Key Laboratory of Advanced Control and Intelligent Automation for Complex Systems, Wuhan 430074, China

^d Faculty of Engineering, China University of Geosciences, Wuhan, Hubei 430074, China

^e Engineering Thermodynamics, Process & Energy Department, Faculty of Mechanical Engineering, Delft University of Technology, Leeghwaterstraat 39, Delft 2628CB, The Netherlands

^f National Center for International Research on Deep Earth Drilling and Resource Development, China University of Geosciences, Wuhan 430074, China

Table S1. Parameters for the TIP4P/ice water model, [1] OPLS-UA methane, [2] and the CLAYFF force field. [3] σ and ε are the Lennard-Jones parameters, in units of nm and kJ/mol, respectively; q is the partial charge of an atom in units of elementary charge (e); m is the atomic mass in units of g/mol

atom	ε / [kJ/mol]	σ / [\AA]	q / [e]	m / [g/mol]
H ₂ O				
O	0.8822	0.31668	-1.1794	16.0
H	0	0	0.5897	1.008
CH ₄	1.23	0.373	0	16.0
Na-				
Montmorillonite				
Si (st)	7.70065×10^{-6}	0.330200	2.1	28.09
Al (ao)	5.56388×10^{-6}	0.427100	1.575	26.98
Mg (mgo)	3.77807×10^{-6}	0.526400	1.3598	24.31
O (ob)	0.650170	0.316556	-1.05	16.0
O (obos)	0.650170	0.316556	-1.1808	16.0
O (oh)	0.650170	0.316556	-0.95	16.0
O (ohs)	0.650170	0.316556	-1.0808	16.0
H (ho)	0.0	0.0	0.425	1.008
Na	1.47545	0.215954	1.0	22.99

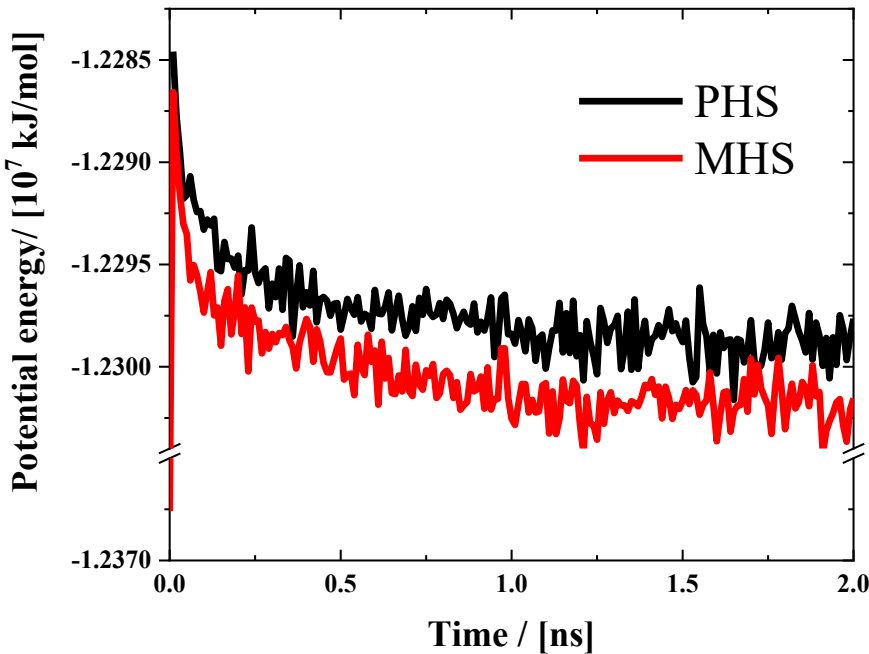


Fig. S1. Time variation of the potential energy for the two systems. Due to the thermostat and barostat, the initial configuration undergoes significant changes. The potential energy rapidly increases, leading to the partial destruction of the hydrate crystal cages. Subsequently, the potential energy slowly decreases until reaching equilibrium, and the hydrate reforms to a stable state of equilibrium.

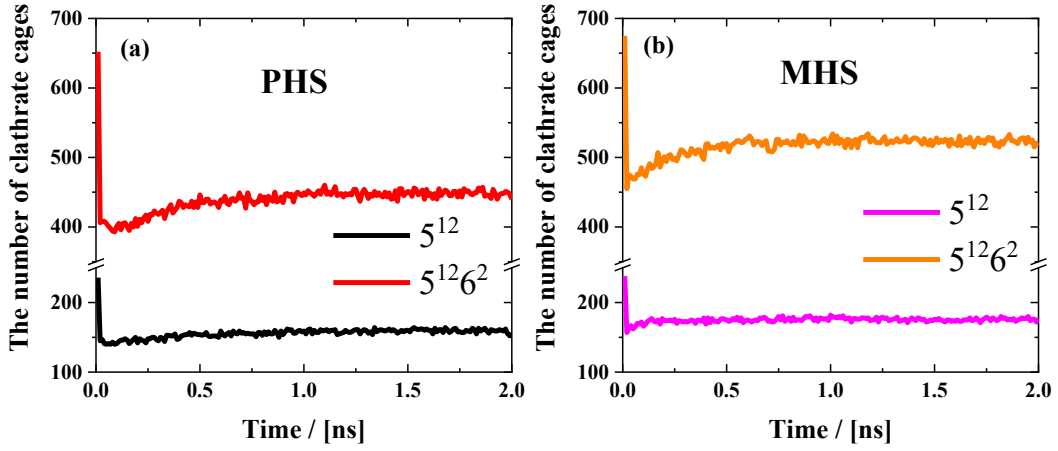


Fig. S2. The number of clathrate cages as a function of time for the two simulation systems (a) PHS, and (b) MHS. This temporal trend is consistent with the potential energy variation shown in Figure S1.

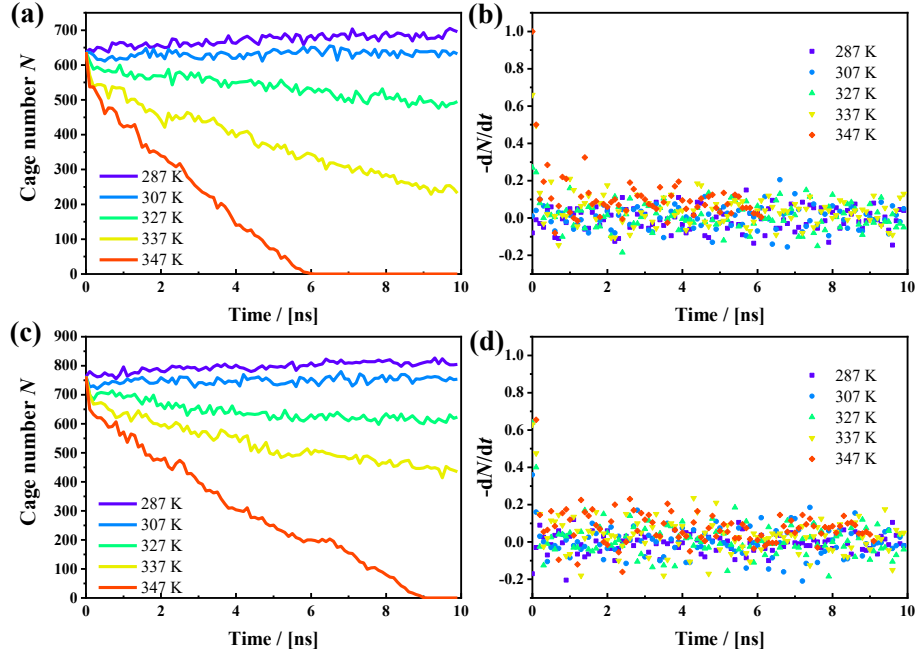


Fig. S3. Time variation total cage number in (a) PHS and (c) MHS system and the cage number negative derivative to time, (b) PHS and (d) MHS

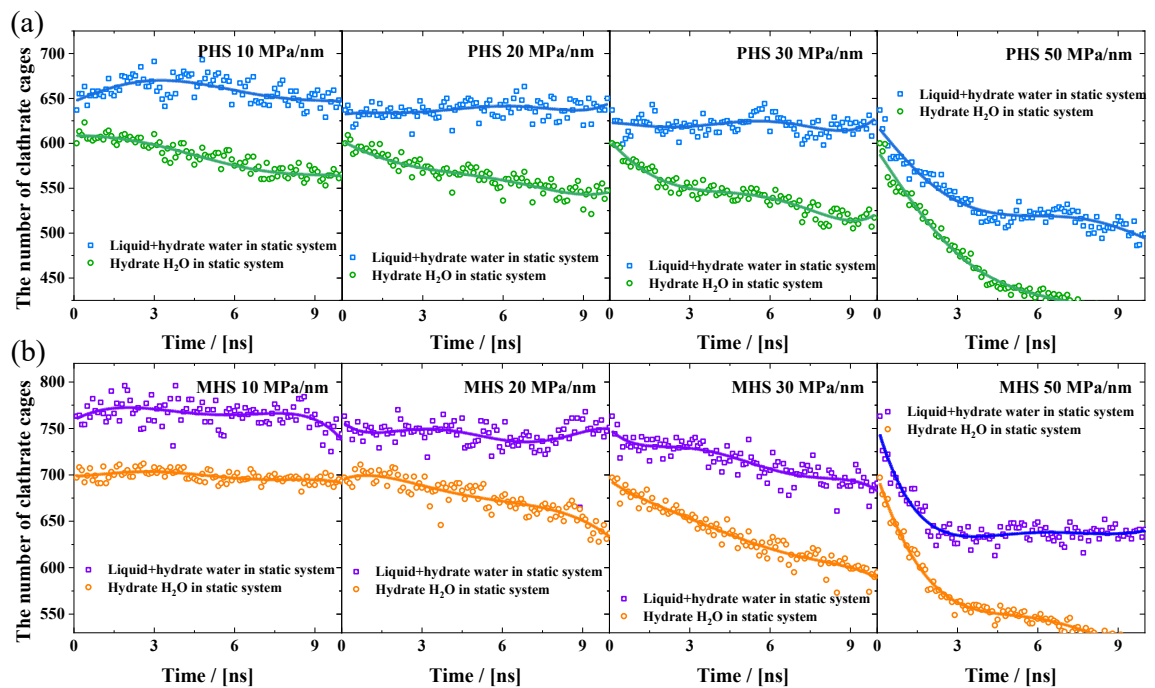


Fig. S4. Time variation of two types of hydrate cage numbers constructed by water in the static system and in the flow system, (a) PHS, (b) MHS

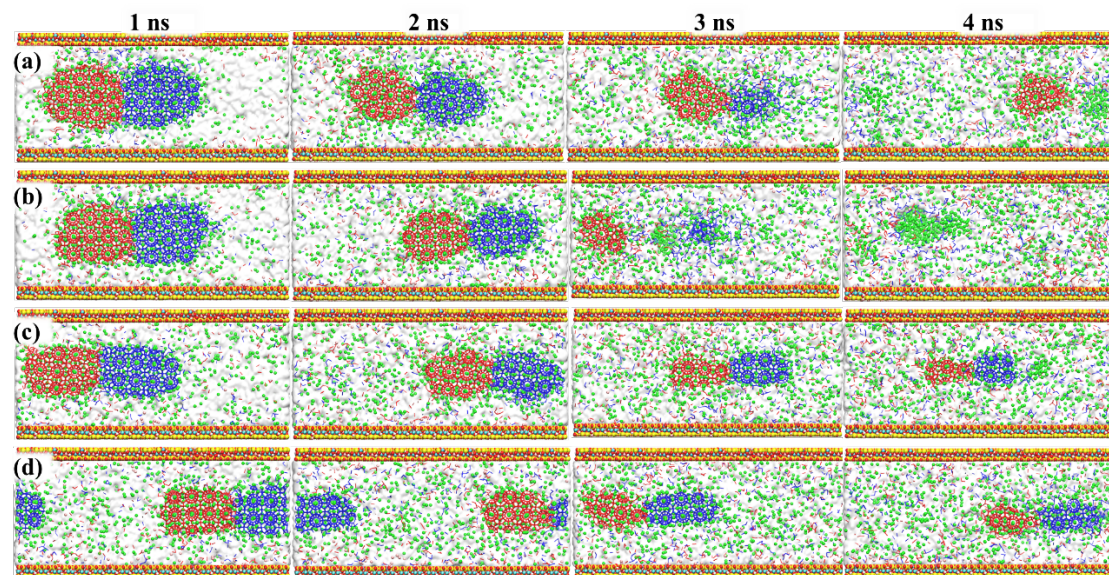


Fig. S5. Snapshots of polycrystalline hydrate dissociation in clay nanopores at 347 K and different pressure gradients: (a) 5 MPa/nm, (b) 10 MPa/nm, (c) 20 MPa/nm, (d) 30 MPa/nm.

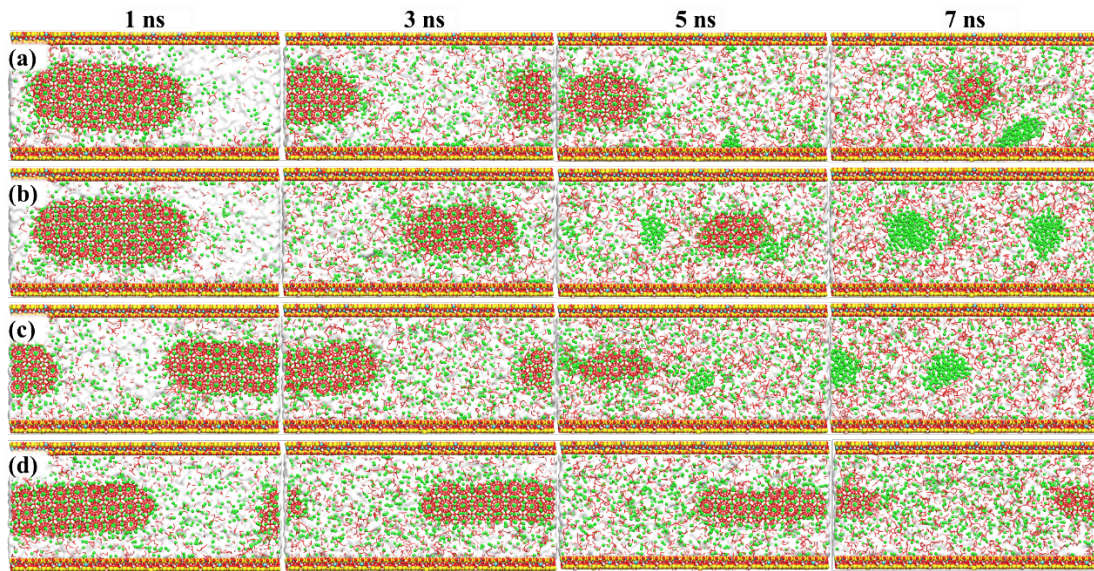


Fig. S6. Snapshots of monocrystalline hydrate dissociation in clay nanopores at 347 K and different pressure gradients: (a) 5 MPa/nm, (b) 10 MPa/nm, (c) 20 MPa/nm, (d) 30 MPa/nm.

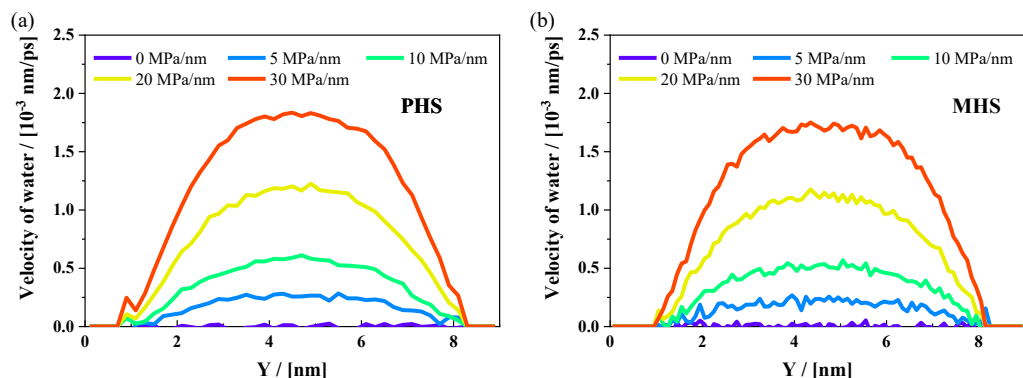


Fig. S7. Velocity profiles of water molecules in clay pores for different pressure gradients for the (a) PHS and (b) MHS systems at 347 K.

- [1] J.L.F. Abascal, E. Sanz, R. García Fernández, C. Vega, A potential model for the study of ices and amorphous water: TIP4P/Ice, *J. Chem. Phys.* 122(23) (2005). <https://doi.org/10.1063/1.1931662>.
- [2] M.G. Martin, J.I. Siepmann, Transferable potentials for phase equilibria. 1. United-atom description of n-alkanes, *J Phys Chem B* 102(14) (1998) 2569-2577. <https://doi.org/DOI 10.1021/jp972543+>.
- [3] R.T. Cygan, J.-J. Liang, A.G. Kalinichev, Molecular models of hydroxide, oxyhydroxide, and clay phases and the development of a general force field, *J. Phys. Chem. B* 108(4) (2004) 1255-1266. <https://doi.org/10.1021/jp0363287>.